

Conformational Change in an Isolated Single Synthetic Polymer Chain on a Mica Surface Observed by Atomic Force Microscopy

Jiro Kumaki*^{†,‡} and Takeji Hashimoto*^{†,§}

Contribution from the Hashimoto Polymer Phasing Project, ERATO, Japan Science and Technology Corporation, Japan, and Department of Polymer Chemistry, Graduate School of Engineering, Kyoto University, Kyoto 606-8501, Japan

Received October 22, 2002; E-mail: kenku@nifty.com; hashimoto@alloy.polym.kyoto-u.ac.jp

Abstract: The random coil conformation of an isolated *conventional synthetic polymer chain* was clearly imaged by atomic force microscopy (AFM). The sample used was a poly(styrene)-*block*-poly(methyl methacrylate) diblock copolymer. A very dilute solution of the copolymer with benzene was spread on a water surface. The structure thus formed on water was subsequently transferred and deposited onto mica at various surface pressures and observed under AFM. The AFM images obtained with films deposited at a low surface pressure (<0.1 mN/m) showed a single polystyrene (PS) block chain aggregated into a single PS particle with a single poly(methyl methacrylate) (PMMA) block chain emanating from the particle. Immediately after the deposition, the single PMMA block chain aggregated to form a condensed monolayer around the polystyrene particles. However, after exposing the deposited film to highly humid air for 1 day, the PMMA chains spread out so that the single PMMA block chain could be identified as a random coil on the substrate. The thin water layer formed on the mica substrate in humid air may enable the PMMA block chain to be mobilized on the substrate, leading to the conformational rearrangement from the condensed monolayer conformation to an expanded and elongated coil. The elongation of the PMMA chain was highly sensitive to the humidity; the maximum elongation was obtained at 79% relative humidity. The elongation was a slow process and took about 20 h.

1. Introduction

The invention of scanning probe microscopy (SPM), such as scanning tunneling microscopy and atomic force microscopy (AFM), has brought us to a stage where we can directly observe individual atoms and molecules. It enables us to manipulate and even to measure directly physical properties of individual atoms or molecules.¹ Furthermore, individual molecules may be manipulated in such a way that an assembly of a small number of molecules can create a particular new function. Along this line, such macromolecules that have a large number of monomer units with various functional groups arranged in a special sequence can create a high functional device and may provide a key for an advanced nanotechnology. For this type of nanotechnology it would be an important first step to be able to directly observe isolated individual macromolecules fixed on a particular substrate of interest.

There have been previous reports of SPM studies of individual isolated macromolecules;² the macromolecules studied so far are limited to “biomacromolecules” such as DNA,³ pectin,⁴ zanthan,⁵ and succinoglycan.⁶ As for synthetic flexible macromolecules with conventional molecular weight, there have been few reports, e.g. our report on poly(methyl methacrylate) (PMMA) deposited on mica substrate.⁷ For recent studies on visualization of isolated synthetic macromolecules, readers may wish to refer to a recent review article by Sheiko and Möller,^{2c} where the SPM images were presented for rigid rodlike polypeptides, monodendrons, single molecular brushes, and so on. However, those isolated macromolecules are much more complex than the flexible and linear PMMA dealt with here.

[†] Japan Science and Technology Corp.

[‡] Present address: Plastics Research Laboratory, Chemicals Research Laboratories, Toray Industries, Inc., 9-1, Ooe, Minato-ku, Nagoya 455-8502, Japan.

[§] Kyoto University.

(1) (a) Wiesendanger, R.; Guntherodt, H.-J., Eds. *Scanning Tunneling Microscopy I, II and III*; Springer: Heidelberg, 1992 and 1993. (b) Bonnell, D. A. *Scanning Tunneling Microscopy and Spectroscopy, Theory, Technique, and Applications*; VCH Publishers: New York, 1993. (c) Magonov, S. N.; Whangbo, M.-H. *Surface Analysis with STM and AFM*; VCH Publishers: New York, 1996.

(2) For a review of scanning probe microscopy works on polymers, see: (a) Chapter 13 in the ref 1c; (b) Tsukruk, V. V.; Reneker, D. H. *Polymer* **1995**, *36*, 1791–1808. (c) Magonov, S. N.; Reneker, D. H. *Annu. Rev. Mater. Sci.* **1997**, *27*, 175–222. (d) Sheiko, S. S. *Adv. Polym. Sci.* **2000**, *151*, 61–174. (e) Sheiko, S. S.; Möller, M. *Chem. Rev.* **2001**, *101*, 4099–4123.

(3) see for example, Hansma, H. G.; Vesenska, J.; Siegerist, C.; Kelderman, G.; Morrett, H.; Sinsheimer, R. L.; Elings, V.; Bustamante, C.; Hansma, P. K. *Science* **1992**, *256*, 1180–1184; Hansma, H. G.; Hoh, J. H. *Annu. Rev. Biophys. Biomol. Struct.* **1994**, *23*, 115–139; Hansma, H. G.; Browne, K. A.; Bezanilla, M.; Bruice, T. C. *Biophys. J.* **1994**, *33*, 8436–8441.

(4) Round, A. N.; MacDougall, A. J.; Ring, S. G.; Morris, V. J. *Carbohydr. Res.* **1997**, *303*, 251–253.

(5) Capron, I.; Alexandre, S.; Muller, G. *Polymer* **1998**, *39*, 5725–5730.

(6) Balnois, E.; Stoll, S.; Wilkinson, K. J.; Buffle, J.; Rinaudo, M.; Milas, M. *Macromolecules* **2000**, *33*, 7440–7447.

(7) Part of this work was previously reported as a communication: Kumaki, J.; Nishikawa, Y.; Hashimoto, T. *J. Am. Chem. Soc.* **1996**, *118*, 3321–3322.

Later AFM studies of isolated PMMA chains on mica revealed that the chains can move on mica in an ordinary laboratory atmosphere. The mobility is believed to be enhanced by adsorbed water on mica and driven by Brownian motion of macromolecule segments. As a consequence, the isolated PMMA chains on mica undergo thermoreversible conformational rearrangements in an effectively two-dimensional space (2D). We here report on the characteristic time for chain conformational rearrangement and its dependence on the relative humidity of the mica/PMMA environment. We will also discuss the fundamental physics underlying this phenomenon with special regard to competing interactions among PMMA, mica, and water. Such studies would be important not only in basic scientific problems concerning 2D conformation of macromolecules but also in controlling their mobility, orientation, and spatial alignment on substrates.

To study polymer chains with SPM, we must fix the molecules on a substrate. Usually this has been achieved by pouring a drop of a very dilute solution of macromolecules on a substrate followed by evaporating the solvent. However, this process requires a very dilute solution in order to prevent macromolecules from aggregation during the solvent evaporation process. As a consequence, an insufficient number of macromolecules are fixed on the substrate, to provide satisfactory statistical accuracy in our observations. To circumvent this difficulty, we applied the Langmuir–Blodgett (LB) method, with which we first spread a dilute solution of macromolecules onto a water surface and then transferred the spread macromolecules onto a mica substrate. This method more carefully controlled the number of macromolecules per unit area being deposited on the substrate.

Immediately after the invention of SPM, it was applied to investigate polymer conformations in polymeric LB films. However, no clear conclusions have yet been reached; for example, Albrecht et al. reported that a LB film of an atactic PMMA did not reveal any clear images concerning conformations of individual isolated chains.⁸ To circumvent some difficulties encountered by the observations, we decided to use a block copolymer, poly(styrene)-*block*-poly(methyl methacrylate) (PS-*b*-PMMA), instead of a PMMA homopolymer. The merit in using the block copolymer will shortly become apparent.

Figure 1 shows a schematic representation of a possible conformation of a single chain of PMMA (a) and of PS-*b*-PMMA (b) spread on a water surface. PMMA has a hydrophilic ester group in its repeating unit and is well-known to spread on water surface as a monolayer with the repeating units being adsorbed on the water surface (part a). PMMA segments are expected to be condensed in the monolayer. In contrast, since polystyrene (PS) has no hydrophilic group, the single PS chain avoids contact with water by collapsing into a particle (gray particle in part b). We will refer to this particle as a *PS single-chain particle*. Moreover, a single PS block chain forming a single PS particle is referred to a *PS monoblock particle* (part b). Thus, as shown in Figure 1b, PS-*b*-PMMA is expected to form a PS monoblock particle from which a single-chain PMMA condensed monolayer is emanated. We anticipated that the PS

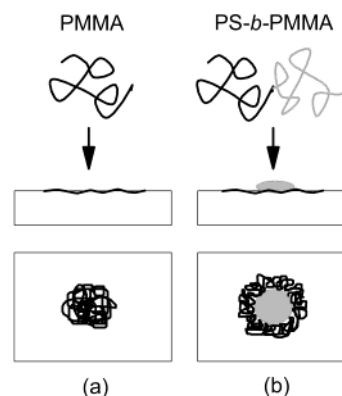


Figure 1. Schematic representation of a PMMA (a) and PS-*b*-PMMA (b) macromolecule spread on a water surface.

monoblock particle could serve as a target particle for observation of single PMMA chains. To attain the isolated PS-*b*-PMMA structure as shown in Figure 1b on a water surface, we used a very dilute solution of block copolymer, typically 4×10^{-6} g/mL, in a solvent, benzene, that spreads on the water surface. The concentration employed was lower than the overlap concentration of polymer by 2–3 orders of magnitude. This approach for obtaining isolated PS-*b*-PMMA block chains is identical to that employed for obtaining the single-chain PS particles.^{9–11}

Immediately after the deposition, however, a single PMMA block chain formed a condensed monolayer around a PS monoblock particle. Though this is a particular conformation that the single PS-*b*-PMMA chain can take, it does not permit us to identify the PMMA segmental units curvilinearly connected along the chain contour. However, after subsequent exposure of the monolayer to highly humid air, the conformation of the PMMA chain was dramatically expanded and elongated on the mica surface, giving rise to a situation where the individual chain segments were isolated from others. This situation fortunately allows us to identify random-coil conformations of isolated PMMA chains on the substrate as described briefly in the previous communication.⁷ In this paper, we report a full description of our experimental results on the conformational change of the PMMA single block chain attached to the PS monoblock particle on the mica surface along with some discussion on the important physical factors underlying this phenomenon.

2. Experimental Section

The block copolymer used, PS-*b*-PMMA, has number-average molecular weights of 1.55×10^5 for PS and 3.92×10^5 for PMMA with the polydispersity index of 1.08 (Polymer Source Inc., Canada). Homopolymers, PS ($M_n = 3.09 \times 10^5$, $M_w/M_n = 1.18$) and PMMA ($M_n = 3.12 \times 10^5$, $M_w/M_n = 1.06$), were used for a surface pressure vs area measurement as a comparison to the block copolymer.

The polymers were spread onto the water surface (purified by Milli-Q system with a low TOC unit, Milli-Q SP Low TOC) at 25 °C by dropping solutions with a polymer concentration of 4×10^{-6} g/mL in benzene (spectroscopic grade) in a commercial LB trough equipped with a Wilhelmy-type film balance (FSD-50, USI). These spreading conditions were similar to those used for obtaining PS single-chain particles.^{9–11}

(8) Albrecht, T. R.; Dovek, M. M.; Lang, C. A.; Grutter, P.; Quate, C. F.; Kuan, S. W. J.; Frank, C. W.; Pease, R. F. W. *J. Appl. Phys.* **1988**, *64*, 1178–1184.

(9) Kumaki, J. *Macromolecules* **1986**, *19*, 2258–2263.

(10) Kumaki, J. *Macromolecules* **1988**, *21*, 749–755.

(11) Kumaki, J. *J. Polym. Sci., Part B, Polym. Phys.* **1990**, *28*, 105–111.

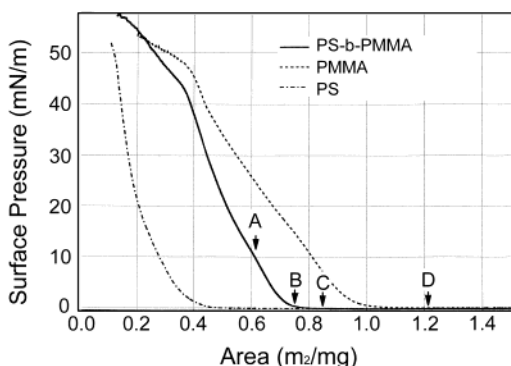


Figure 2. Surface pressure vs area curves of PS-*b*-PMMA, PS, and PMMA. The AFM samples of PS-*b*-PMMA were transferred from the water surface and deposited onto mica at the areas indicated by the arrows A–D.

The single layer of block copolymer that formed on the water surface at various constant surface pressures was deposited onto freshly cleaved mica by pulling the mica out of the water surface at the rate of 4 mm/min (the vertical dipping method). The transfer ratio (the decrease in monolayer area on water during the deposition)/(the area of the substrate) was 1 ± 0.05 for the deposition at the surface pressure of 1 and 10 mN/m and 1.2 at the surface pressure of 0.2 mN/m, respectively. In addition, to observe isolated individual molecules the monolayers were transferred onto the substrate before they could coalesce into a continuous film. The typical area at the deposition was $1.7A_0$, where A_0 is the limiting area determined from the surface pressure vs area curve, as will be discussed in section 3.1. In this case, the surface pressure at the deposition was less than 0.1 mN/m, so that the area and transfer ratio were not well determined. However AFM results showed that the deposition was reproducible.

The deposited monolayers on mica were observed in air by a tapping mode AFM (NanoScopeIII, Digital Instruments) with a silicon cantilever (resonance frequency 300–400 kHz, spring constant 70–90 N/m). AFM images are shown in the height mode without any image processing except flattening. The samples were observed by AFM immediately after the deposition and also after sample exposure to highly humid atmosphere. Humidity was controlled by enclosing the samples with a water solution in a container. The water solutions used were pure water (for 100% relative humidity (RH)) and pure water saturated with Na_2CO_3 (yielding 87% RH), with NH_4Cl (yielding 79.3% RH), and with $\text{NH}_4\text{Cl} + \text{KNO}_3$ (yielding 71.2% RH). The AFM observation was done in the laboratory condition at the relative humidity of 50–60%.

3. Results and Discussion

3.1. Structure of LB Film Deposited at 10 mN/m and Identification of PS Monoblock Particles. Figure 2 shows the surface pressure vs area curve for the block copolymer along with those for PS and PMMA homopolymers. PMMA, which spreads on water surface as the monolayer, shows a relatively expanded curve, while PS, which does not spread on water surface, shows a compressed curve. The pressure vs area curve for the block copolymer was intermediate between them. The conventional linear extrapolation of the high-pressure limb of the curve to zero pressure yields limiting areas, A_0 , which was $0.71 \text{ m}^2/\text{mg}$ for PS-*b*-PMMA, $0.94 \text{ m}^2/\text{mg}$ for PMMA, and $0.24 \text{ m}^2/\text{mg}$ for PS, respectively.

Figure 3 shows AFM image for the block copolymer film transferred onto mica at the surface pressure of 10 mN/m; the deposition condition is indicated with the arrow A on the surface pressure vs area curve in Figure 2. Small particles with a relatively narrow distribution in size, indicated by the arrows A, were observed, while some particles are isolated, others are

interconnected to form stringlike arrays. There are also large particles indicated by the arrows B. As will be discussed later, we can conclude that the small particles are the PS monoblock particles, and the large particles are PS-*b*-PMMA multiblock particles, i.e., the particles composed of many PS-*b*-PMMA block chains. Though beyond the scope of the present paper, it may be intriguing to explore the internal structure of these large particles, if there were any, from a viewpoint of microphase separation of PS-*b*-PMMA in this special confined space.

Detailed investigations of the image revealed the following features: the small particles have diameter of 11–15 nm and a thickness of 2.5 nm; these particles are on the PMMA monolayer with a thickness of 1 nm, as schematically shown in Figure 3b.¹² A fast Fourier transform (FFT) of the image showed a peak intensity, the wavenumber of which corresponds to an average particle–particle spacing of 45 nm. This regular spacing is due to the PMMA condensed monolayer that emanated from and intervened between the PS particles.

The small particles were identified to be comprised of a single PS block chain from the following two points. Assuming the PS monoblock particles are compressed to an oblate ellipsoidal shape with the measured thickness of 2.5 nm and have the same density as the bulk PS (1 g/cm^3), we can estimate the diameter of the particles from the molecular weight of the PS block. The value estimated is 14 nm, in good agreement with the observed diameters. The identification is also made possible from the reasonable number of the particles in the image. The number of particles in the image shown in Figure 3 is 303, including the large ones. From our deposition conditions, and assuming that the molecules are homogeneously distributed throughout the film, we expect 420 PS monoblock particles to be deposited in the same sample substrate area. Thus, each particle in Figure 3 contains 1.4 molecules in average. Taking into account the presence of multiblock particles and the fact that the molecules on the water surface may not have been perfectly distributed, we may conclude the small particles in Figure 3 are the PS monoblock particles.

Lennox and Eisenberg et al.¹³ have reported studies of micelle formation for some block copolymers on a water surface. For example, by spreading a poly(styrene)-*block*-poly(butyl methacrylate) (PS-*b*-PBuMA) on a water surface, they observed regular aggregates consisting of a central core of PS blocks from which the PBuMA monolayer emanated. However, the core contained several hundred PS blocks. The main differences between their experiments and ours are as follows: they used relatively high concentrations of the block copolymer solutions ($5 \times 10^{-4} \text{ g/mL}$, cf. $4 \times 10^{-6} \text{ g/mL}$ in this work) in a different solvent (chloroform, cf. benzene in this work) and low molecular weight samples [$M_n = (2.9\text{--}6.3) \times 10^4$, cf. $M_n = 5.47 \times 10^5$ in this work]. Therefore, their work refers to a different regime of block copolymer assembly.

We obtained the PS monoblock particles. However, PMMA molecules around the particles formed, by and large, a continu-

- (12) The precise measurement of the particle diameter is difficult due to the finite tip size effect in AFM measurement. We discuss our approach to overcome this difficulty in section 3.2.
- (13) For an example of surface micelle formation of nonionic block copolymers, see: Li, S.; Hanley, S.; Khan, I.; Varshney, S. K.; Eisenberg, A.; Lennox, R. B. *Langmuir* **1993**, *9*, 2243. For their previous works with block polyelectrolytes, see: Zhu, J.; Eisenberg, A.; Lennox, R. B. *J. Am. Chem. Soc.* **1991**, *113*, 5583–5588. Zhu, J.; Lennox, R. B.; Eisenberg, A. *J. Phys. Chem.* **1992**, *96*, 4727–4730. Zhu, J.; Eisenberg, A.; Lennox, R. B. *Macromolecules* **1992**, *25*, 6547–6555.

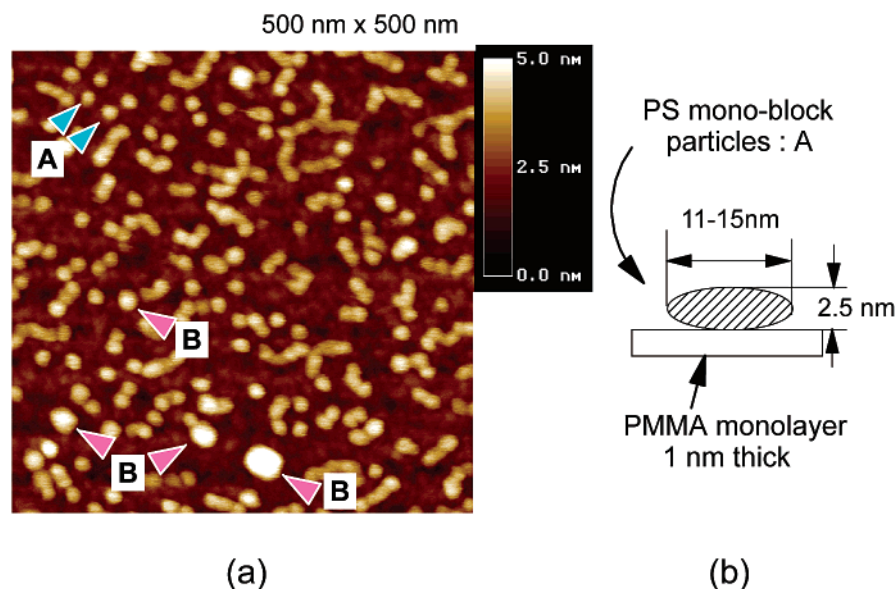


Figure 3. AFM image of a PS-*b*-PMMA film deposited on mica at a surface pressure of 10 mN/m (a). The arrows A in part a indicate the PS monoblock particles; the sizes of them are schematically shown in part b with the PMMA monolayer beneath the particle. The arrows B in part a indicate larger particles that contain more than one PS-*b*-PMMA block. The FFT shows a regular particle–particle spacing (45 nm) which is due to the PMMA monolayer emanated from and intervened between the PS particles.

ous matrix throughout the monolayer and hence could not be seen as an isolated single chain even at this stage. To observe PMMA molecules around the particles, we tried to deposit isolated monolayers of PMMA by reducing the surface pressure in the LB trough during deposition.

3.2. Structure of LB Films Deposited at Lower Surface Pressures. Figure 4 shows AFM images of PS-*b*-PMMA LB films deposited at surface pressures of (A) 10, (B) 1, (C) 0.2, and (D) less than 0.1 mN/m; the deposition conditions of the images A–D are indicated by the arrows (A–D) in the surface pressure vs area curve in Figure 2, respectively. The PS monoblock particles having high heights from the substrate are shown in pink and the PMMA monolayer having a low height is shown in light blue. Upon decreasing the surface pressure at the deposition, the number density of the PS particles is reduced, and at a surface pressure of 0.2 mN/m (C) there appear voids in the PMMA monolayer. At a surface pressure of less than 0.1 mN/m (D), the PS monoblock particles (pink) surrounded by the condensed PMMA monolayers (light blue) are dispersed on the bare mica surface (dark blue).

In Figure 5a (the same image as Figure 4D), the particles marked by A, B, and C are isolated PS monoblock particles. They tend to aggregate to form stringlike structures, as shown by the objects marked by D, E, F, G, and H. For example, as shown in the contrast-enhanced and enlarged image of Figure 5b, the stringlike structure D and E contains five and three PS monoblock particles, respectively. These particles or strings are surrounded by the condensed PMMA monolayer (thickness 0.2–0.5 nm). A small number of large particles shown by the objects marked by I, J, and K are the multiblock particles that could be easily distinguished from the smaller and thinner PS monoblock particles. The particle A contains only one PS monoblock particle; thus, the structure is composed of a single PS-*b*-PMMA molecule isolated from others.

3.3. Structure of a Single PS-*b*-PMMA Molecule Isolated from Other Molecules. Figure 6a shows a height profile of the particle along the scanning direction shown by the yellow

line (part b), and the observed results are schematically summarized in part c. The thickness of the PS monoblock particle and the PMMA monolayer relative to the mica surface are ca. 2.5 and 0.2–0.5 nm, respectively. On the other hand, the thickness of PS monoblock particles deposited at 10 mN/m was 2.5 nm from the surface of the 1.0-nm-thick PMMA monolayer (see Figure 3). Thus, at the lower surface pressure, the PMMA monolayer existed outside of the PS monoblock particles, but upon increasing the surface pressure, the PMMA monolayer was compressed to a continuous film that squeezed out the PS monoblock particles on top of the condensed PMMA film.

In AFM observations, the lateral size of the PS particles may be enlarged due to the finite size of the probe tip, but the particle–particle distances and the particle height are essentially unaffected by this, if the distances are larger than a critical value.¹⁴ In the present work, the diameters of the particles are measured precisely from the distances between contacting particle centers. Figure 7 shows the height profiles of the aggregate of G in Figure 5a. The aggregate G is found to be an array of four PS monoblock particles, as shown in the height profile of part b, which is taken along the scanning line β in the AFM image shown in part c. The diameter of a single particle forming the aggregate may be estimated as the distance between the two arrows marked by number 2 in part a, which is taken along the scanning line α shown in part c. The value thus estimated is 27.8 nm, much larger than that expected (14 nm) for the PS monoblock particles, which is due to the finite tip size effect. On the other hand, the particle–particle distances measured as the distances between the two sets of arrows marked by numbers 3 and 4 in the height profile shown in part b obtained along the scanning line β in the image shown in part c are all 14.9 nm, in good agreement with the diameter expected for the PS monoblock particles. The thickness of the PS monoblock particle is 2.54, as measured by the vertical

(14) Markiewicz, P.; Goh, M. C. *Langmuir* **1994**, *10*, 5–7.

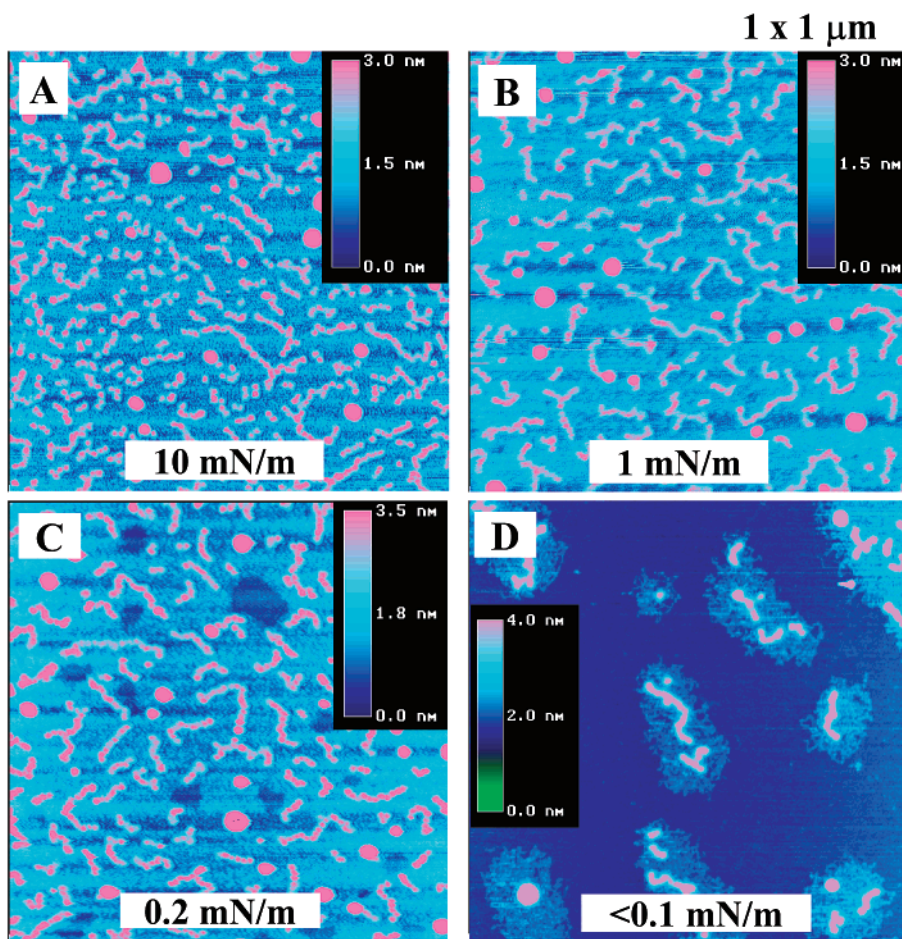


Figure 4. AFM images of PS-*b*-PMMA monolayers deposited on mica at surface pressures of (A) 10 mN/m, (B) 1 mN/m, (C) 0.2 mN/m, and (D) less than 0.1 mN/m, respectively. The PS particles are shown by pink, the PMMA monolayers are shown by light blue, and the bare mica surface is shown by dark blue.

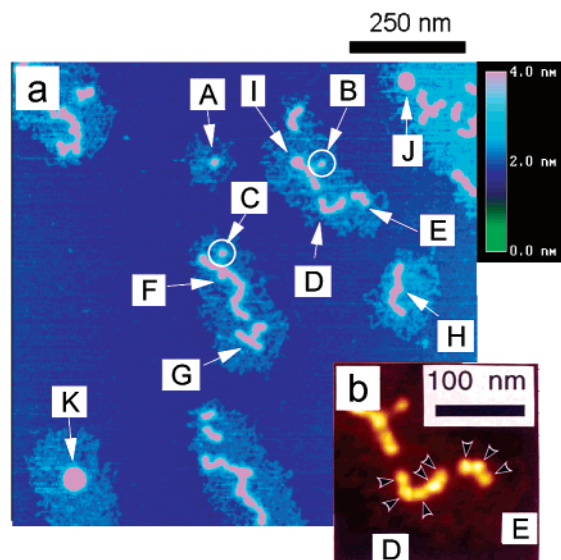


Figure 5. (a) AFM image of a PS-*b*-PMMA film deposited on mica at a surface pressure of less than 0.1 mN/m and at an area of $1.7A_0$ for the block copolymer. (b) An enlarged and contrast-enhanced image of the stringlike structures of D and E in part a, which are composed of five and three PS monoblock particles, respectively, as indicated by the arrows.

distance between the two arrows numbered 1 in the height profile shown in part a, and is not affected by the finite tip size.

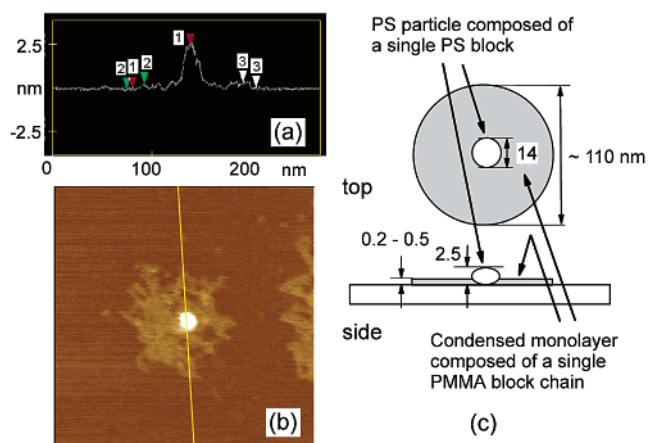


Figure 6. (a) Height profile along the line indicated in the image shown in part b, which represents the condensed monolayer composed of a single PS-*b*-PMMA molecule. This image is identical to the part of the image marked by A in Figure 5a. The vertical distance between the two arrows marked by 1 is 2.5 nm, that of the arrows marked by 2 is 0.29 nm, and that of the two arrows marked by 3 is 0.32 nm. (c) A schematic representation of the condensed monolayer composed of the single PMMA block chain.

We can count the number of PMMA molecules participating in the aggregates from the number of the PS monoblock particles. For example, the aggregates A, C + F + G, and H in Figure 5 should contain 1, 21 ± 1 , and 9 molecules, respectively. In Figure 8, the area occupied by PMMA blocks in the aggregate

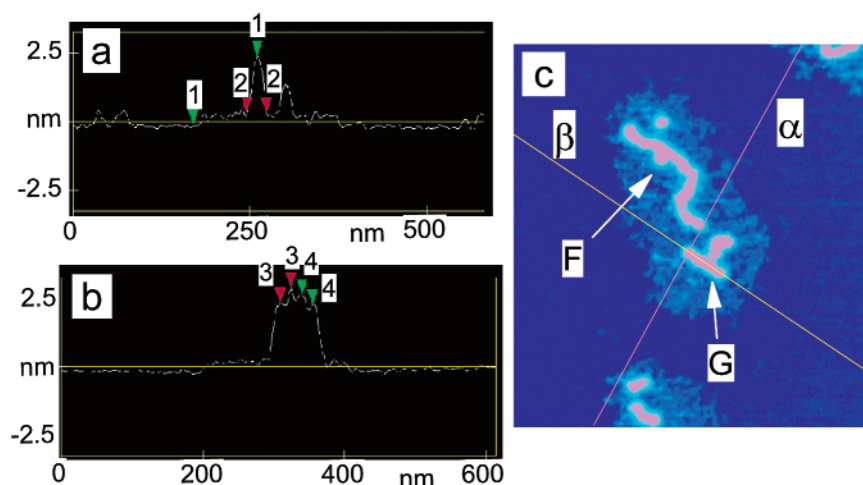


Figure 7. Height profiles along the scanning lines α (part a) and β (part b) on the image shown in part c. The vertical distance between the two arrows marked by 1 in part a is 2.54 nm. The horizontal distance between the two arrows marked by 2 in part a (an apparent diameter) is 27.8 nm. This value is much larger than the value expected for the PS monoblock particles, due to smearing caused by the finite size of the probe tip, while the three horizontal distances between the two sets of arrows marked by 3 and 4 (i.e., 3–3, 3–4, and 4–4 particle–particle distances) are all 14.9 nm, in good agreement with that expected (14 nm) for the diameter of PS monoblock particles.

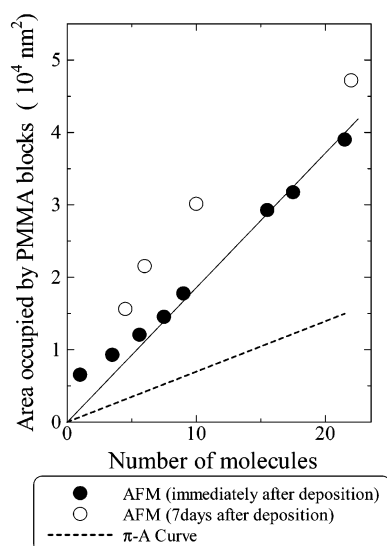


Figure 8. Areas occupied by the PMMA blocks in the aggregates of PS-*b*-PMMA are plotted against the number of the molecules in the aggregates. The filled circles indicate the areas immediately measured after the film deposition on mica, and the open circles indicate the area measured 7 days after the deposition. Note that the PMMA blocks are slowly expanding after the deposition under the laboratory conditions. The dotted line shows the relation between the area and the number of molecules estimated from the limiting area, $A_{0,\text{PMMA}}$, on water surface as measured from pressure vs area curve.

are plotted against the number of the PMMA molecules in the aggregate. The areas are measured immediately after deposition of the film on mica. The area occupied by PMMA blocks clearly increased as the number of molecules in the aggregates increased, and it became proportional to the number of molecules when the number is larger than 10. From the linear relation, the area occupied by a single PMMA block chain is estimated to be $2.0 \times 10^3 \text{ nm}^2/\text{PMMA block}$. The dotted line shows the relation ($6.96 \times 10^2 \text{ nm}^2/\text{PMMA block}$) expected from the limiting area ($A_{0,\text{PMMA}}$) determined from the surface pressure vs area curve of the PMMA homopolymer. The area directly determined by AFM is 2.9 times larger than that expected from $A_{0,\text{PMMA}}$. This implies that the monolayer had expanded after the deposition onto mica. The conformation of

PMMA chains in monolayers on a water surface differs from that on a mica surface. Actually, the thickness of the PMMA block monolayer deposited on mica in Figure 5 (0.2–0.5 nm) is much thinner than the thickness reported for the PMMA monolayer on a water surface as determined by in situ neutron reflectivity (1.5–1.8 nm)¹⁵ and by ellipsometry (1.4 nm).^{16,17}

From Figure 8 we see that the area occupied by the single PMMA block in the aggregates with the number of the molecules smaller than six is significantly larger compared with that in the aggregates with the number of molecules greater than 10. This may correspond to the fact that the PMMA chains having more free area available can expand more easily, probably due to interactions of PMMA chains with other chains and/or mica. Note that while parts of a PMMA chain near the central core of the PS block particle are too compressed to be seen separately from other parts of the chain, parts of the PMMA chain located far apart from the central core are clearly seen in the form of tails or loops. For example, see the tails and loops of the PMMA chain at the left side of the aggregate H in Figure 5.

Using PS monoblock particles as a probe, we can precisely determine the area occupied by PMMA chains. The open circles in Figure 8 show the area of the PMMA blocks measured after keeping the deposited film at a relative humidity of about 54% for 7 days. Surprisingly, the PMMA molecules slowly expanded by about 50%, as a consequence of which the thickness was reduced to 0.2–0.3 nm. This surprising result indicates that the high molecular weight polymer chains are mobile even after the deposition on the substrate. This unexpected finding stimulated us to think that if we accelerate the mobility of the molecules by keeping the samples in highly humid air, we may expand the molecules further so that segments in a given polymer chain are separated from each other, enabling us to

(15) Henderson, J. A.; Richards, R. W.; Penfold, J.; Shackleton, C.; Thomas, R. K. *Polymer* **1991**, *32*, 3284–3294.

(16) Sauer, B. B.; Yu, H.; Yazdaniyan, M.; Zografii, G.; Kim, M. W. *Macromolecules* **1989**, *22*, 2332–2337.

(17) We think this expansion of the surface area in the monolayer during the deposition process occurs only at the deposition from a dilute state or a low surface pressure. The area should be reduced and kept constant at the deposition from a compressed film, such as shown in Figure 3.

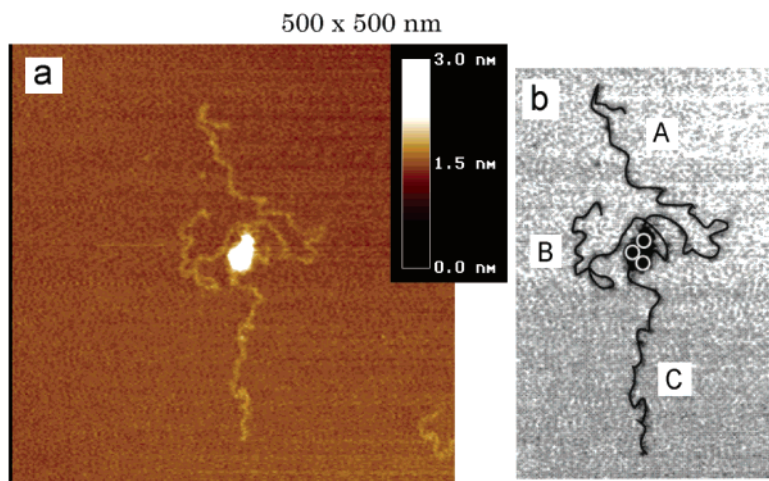


Figure 9. (a) AFM image of a PS-*b*-PMMA deposited on mica under the same conditions as in Figure 5. However, the AFM observation was done after keeping the sample in 100% RH air for 1 h and further 79.3% RH for 26 h. (b) A sketch of the molecular conformations of the PMMA blocks and PS monoblock particles. The image shows conformations of three PS-*b*-PMMA block copolymers.

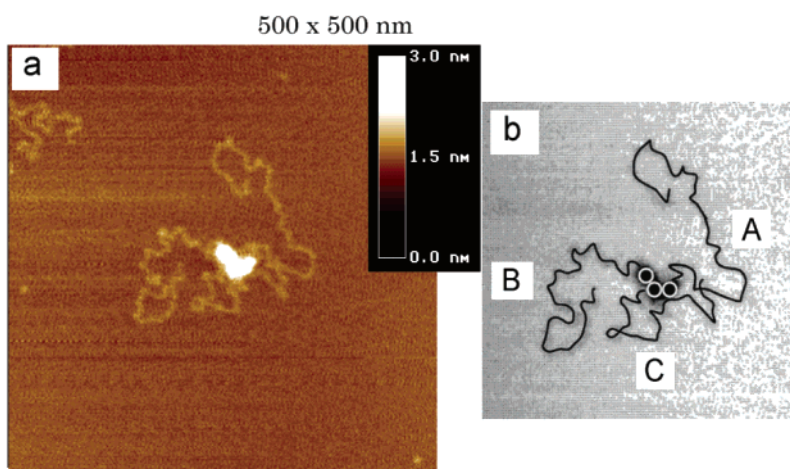


Figure 10. (a) Another representative AFM image for the same sample as in Figure 9. (b) A sketch of molecular conformations. The curvilinear lengths of the lines are A, 503; B, 455; and C, 350 nm. The end-to-end distances are A, 90; B, 63; and C, 66 nm.

see individual chains. Therefore, we have systematically studied the humidity effect.

3.4. Enormous Expansion of PMMA Block Chain on Mica under Humid Air and Direct Observation of Conformations of Single PMMA Block Chains. One of the most expanded conformations of single PMMA chains observed in this work is shown in Figure 9a. This is an AFM image of a sample deposited on mica under the same conditions as in Figure 5, but observation was done after first keeping the sample in a container at 100% RH air for 1 h and subsequently transferring it to another container at 79.3% RH air for 26 h. The condensed PMMA monolayer around the three PS monoblock particles was dramatically expanded into three stringlike conformations. Figure 9b shows a sketch of molecular conformations of PMMA chains. The central core is composed of three PS monoblock particles from which emanate three PMMA block chains.

The curvilinear lengths along PMMA molecules are 549 nm for the chain marked by A, 403 nm for B, and 314 nm for C. From the molecular weight, the length of the fully stretched PMMA block is expected to be ≈ 980 nm [$=Na \sin(\theta/2)$, where N , a , and θ are the number of C–C bonds in the main chain (7840), the C–C bond length (0.154 nm), and C–C–C bond angle (109.3°), respectively]. The observed curvilinear length

should be shorter than the length expected, because small kinks of chains parallel and perpendicular to the substrate are all ignored due to the limited resolution of AFM; the lengths observed here agree within an order of magnitude. We conclude that these strings are PMMA chains, because the number of the PS particles and the strings are the same and the lengths are reasonable from the molecular weight. The end-to-end distances of PMMA block chains are easily determined as 122 nm for the chain marked by A, 73 nm for B, and 189 nm for C.

Figure 10a shows a different aggregation on the same sample. This aggregate is also composed of three block copolymer molecules; molecular conformations are sketched in Figure 10b. Figure 11a shows another example of the AFM images. Although some part of the conformations are difficult to assign, we believe the aggregate is composed of two block copolymer molecules, the conformations of which are sketched in Figure 11b. Note that the chain indicated by C in the figure is unattached to the PS monoblock particle; thus, it seems to be a part of a PMMA chain disrupted from others. From the fact that a PMMA chain free from the PS particle can be seen in the AFM image, we now believe that the existence of a PS block is not the essential prerequisite for observation of isolated single PMMA chains.¹⁸

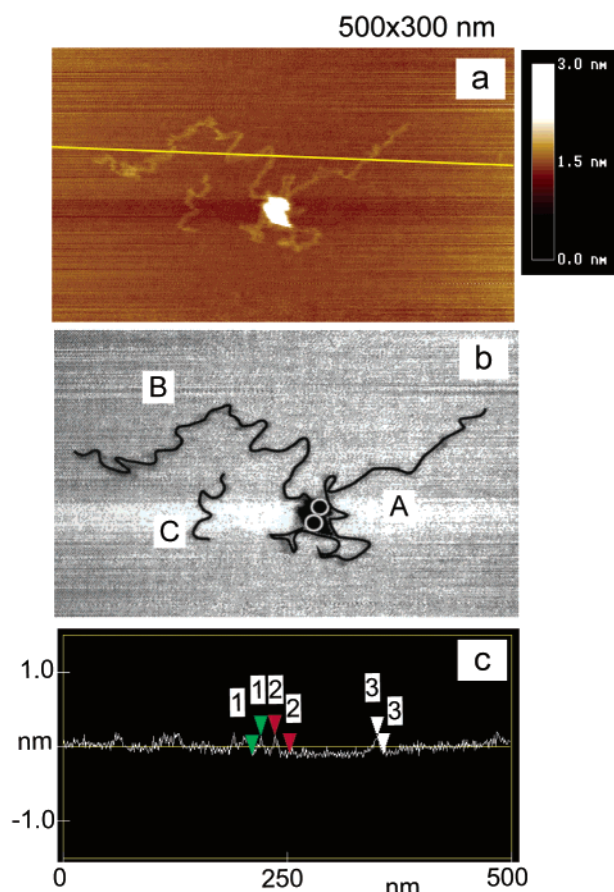


Figure 11. (a) Another representative AFM image for the same sample as in Figure 9. (b) A sketch of molecular conformations. Note that the chain indicated by C seems to be a part of a disrupted PMMA chain. The curvilinear lengths of the lines are A, 507; B, 463; and C, 117 nm. The end-to-end distances are A, 181; B, 198; and C, 60 nm. (c) The height profile of the PMMA chains along the scanning line as indicated in part a.

Figure 11c shows the height profile of the PMMA chains in Figure 11a along the line indicated in part a. The heights between the two arrows numbered 1 and 1, 2 and 2, and 3 and 3 are 0.24, 0.26 and 0.23 nm, respectively, with a noise level of 0.1 nm. The observed chain height is reasonably consistent with the PMMA chain, although it is slightly lower than the van der Waals radius of the chain (around 0.4 nm). On the other hand, the width of the string is about 10 nm, the large value of which is due to the smearing effect arising from the finite tip size (ca. 10 nm). If the amorphous chain is aggregated to form a condensed monolayer with the intersegment distances less than the tip size, no meaningful image will be obtained to identify a single chain entity. This is why previous attempts to observe amorphous monolayers were not successful.⁸ One of the key points for the observation of single chain conformations of PMMA molecules in this study was due to the success in expanding the chain conformations and isolating a part of chain segment from other parts by keeping the chains on mica under the humid air.

Figure 12a shows a histogram of the curvilinear length of the single chains as determined by AFM for 21 PMMA block chains. The lengths are from 200 to 600 nm, which is 20–61% of the fully stretched PMMA chain. Figure 12b shows the end-to-end distance distribution. The average root-mean-square end-

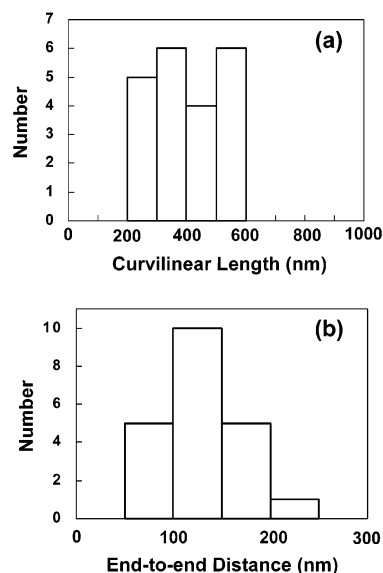


Figure 12. Histogram of the curvilinear length (part a) and the end-to-end distance (part b), directly determined with AFM for 21 PMMA block chains.

to-end distance was 132 nm; this is 4 times larger than expected for the ideal chain of the same PMMA molecule in two-dimensional space (32.7 nm).¹⁹ This quite large expansion is unusual for nonionic polymers. The conformations may reflect interactions among PMMA segments, mica, and the adsorbed water layer on the mica, as will be detailed later in section 3.7.

Figure 13 shows the change in PMMA conformations with time during the period when the deposited film was kept under highly humid air. The deposited film on mica was first kept under 100% RH air for 1 h and then transferred in the chamber kept at 79.3% RH. Further exposure and observation was performed for a range of times, as indicated in the figure. The expansion of PMMA chains is a slow process, and it takes more than 20 h for the chains to be spread so that individual chains can be discerned. The small defects typically shown in Figure 13 after 20 h exposure are small dust particles accumulated during the repeated AFM observations.

3.5. Degree of Chain Expansion on Mica as a Function of Relative Humidity. The expansion of PMMA chains was highly sensitive to the humidity. Figure 14 shows typical examples demonstrating the humidity dependence of PMMA chain expansion. The expansion under a lower humidity of 71.2% RH for 25 h is as small as that under a higher humidity of 100% RH for 48 h. Note that much higher expansion was observed at 79.3% RH (see Figures 9–11 and 13). It is well-known that there is a thin adsorbed water layer on a substrate surface, the thickness of which depends on the relative humidity of the atmosphere. Beaglehole et al. measured the thickness of the adsorbed water layer on mica surfaces as a function of humidity; the thickness was 0.25 nm for 60% RH, 0.35 nm for 71.2% RH, 0.5 nm for 79.3% RH, and 0.8 nm to infinite for 100% RH.^{20,21} Our experimental observation reveals that the thickness of the water layer should strongly affect the chain expansion. We shall discuss possible physical factors underlying this observation later in section 3.7.

(18) Hashimoto, T.; Okumura, A.; Tanabe, D. To be submitted.

(19) Brandrup, J.; Immergut, E. H. *Polymer Handbook*, 3rd ed.; Wiley Publications: New York, 1991.

(20) Beaglehole, D.; Radlinska, E. Z.; Ninham, B. W.; Christenson, H. K. *Phys. Rev. Lett.* **1991**, *16*, 2084–2087.

(21) Beaglehole, D.; Christenson, H. K. *J. Phys. Chem.* **1992**, *96*, 3395–3403.

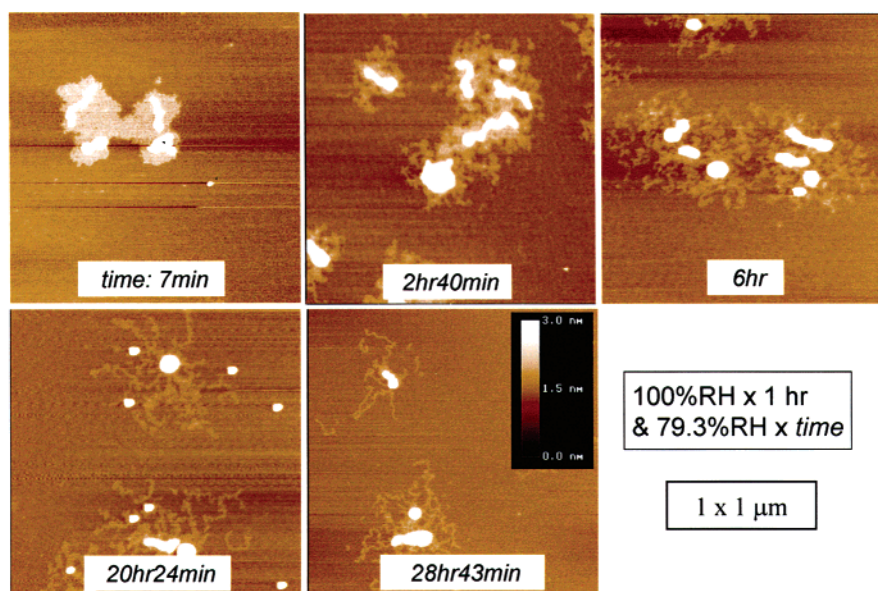


Figure 13. AFM images of a PS-*b*-PMMA monolayer after keeping under humid air for different times. A deposited monolayer on mica under the same conditions as Figure 5 was first kept under 100% RH air for 1 h and subsequently kept under 79.3% RH air for the time indicated in each image. The original magnifications of the images obtained after 7 min, 2 h and 40 min, 6 h, and 20 h and 24 min exposition of the specimen under 79.3% RH were half of that obtained after 28 h and 43 min; they are enlarged by image processing to fit the size to that of 28 h and 43 min. Thus the clarity of the former four images are somewhat reduced. The color scale is the same for all images.

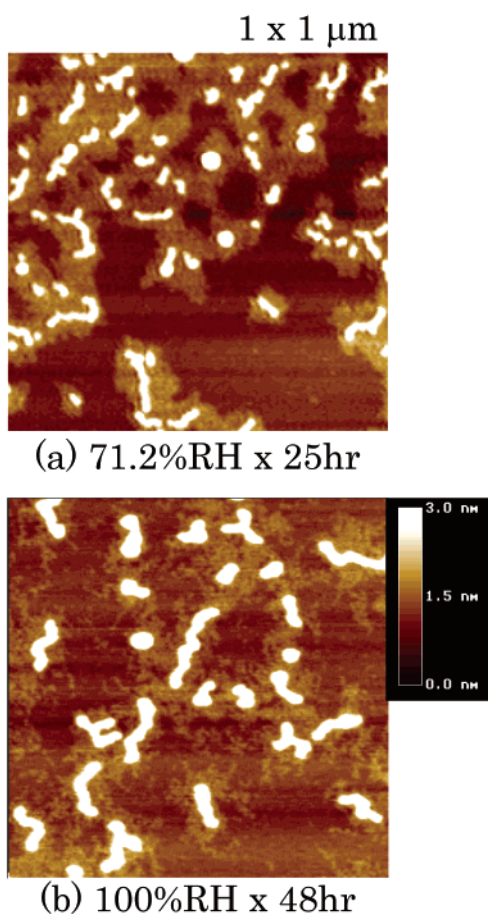


Figure 14. AFM images of a PS-*b*-PMMA film deposited on mica under the same conditions as those employed for Figure 5. The AFM observations were done after keeping the sample under 71.2% RH for 25 h (part a) and 100% RH for 48 h (part b). The color scale is the same for both images.

At 100% RH in Figure 14, some scissions of PMMA chains were visible. This is commonly observed when the samples were

treated under highly humid air (higher than 87% RH) for a long time. The reason is not clear at this moment, but we tentatively speculate as follows. Parts of the chain adsorbed on mica are firmly anchored, but other parts are not. The unanchored parts tend to be driven onto the water surface and are highly mobile, tending to pull the chain against the anchored points. The stress exerted on the chain may give rise to the chain scission.

The chain was expanded at certain humidity conditions. A question arises as to whether this expanded conformation on the mica surface can contract again when the relative humidity is changed. We observed a sample that was once expanded to a maximum extent at 79.3% RH and then further exposed to 100% RH for 17 h, and we confirmed that the PMMA chains were aggregated again. Thus, the chain conformation appears to reversibly change with a change in relative humidity or with a change in the thickness of the water layer on the mica surface. This seems to indicate that the thickness of the water layer on the mica may play a major role. Later, in section 3.7, we will discuss possible physical factors causing this phenomenon.

3.6. Stability of Chain Conformation During AFM Observation. It is important to confirm that the PMMA chain did not alter its shape due to AFM tip manipulation. Figure 15 shows two AFM images of the same area and the same molecules during repeated AFM observations. The sample was first expanded to a maximum extent at high humidity and then kept under the laboratory conditions (50–60% RH) during the observation. As shown in the sketch in part c, the aggregate is composed of about 11 block copolymer molecules. Due to the overcrowding of the PMMA chains in the aggregate, only four chains are clearly assigned as indicated with thick lines (A–D) in part c; some possible chain arrangements for other chains are shown as thin lines. As shown in the figure, there is no visible difference between the conformations observed in the first scan and those observed in the fifth scan obtained 17 min after the first scan. We have observed this aggregate even in

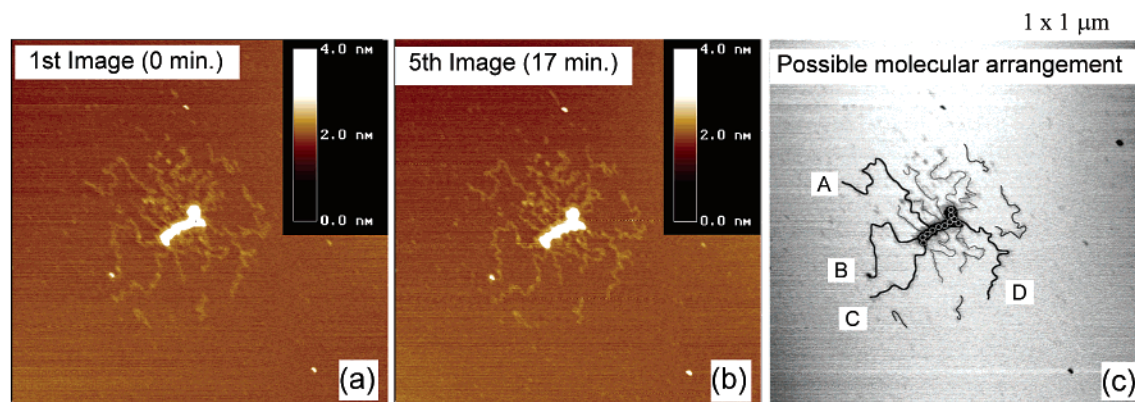


Figure 15. AFM images of a PS-*b*-PMMA film that shows an expansion of the PMMA block chains under the conditions similar to those employed for Figures 9–11. Molecular conformations are shown in the schematic representation in part c. This assembly is composed of about 11 block copolymer molecules. Due to the overcrowding of many molecules, only four PMMA block chains are clearly assigned, as indicated by four thick lines (A–D). Two AFM images in parts a and b show the same molecules during a repeated AFM scanning. There are no visible differences between the conformations at the first AFM scan (part a) and the fifth scan after 17 min (part b).

the 14th scan obtained 4 h after the first scan. There were no visible differences in the observed PMMA conformations. On the other hand, the PS particles, being more fragile, were deformed gradually in the later observations. This indicates that PMMA chains on the mica surface are very stable for AFM observation and that molecular motion is frozen in the time and length scale of this observation under the given RH.

3.7. Possible Physical Factors Underlying the Conformational Change of Isolated Single PMMA Chains on the Mica Surface. After transferring and deposition of the LB films on water at low surface pressure onto mica, we could identify isolated single block copolymer chains that formed a condensed monolayer of a single PMMA block around the PS monoblock particle (see Figure 6). This particular conformation of the PMMA block is shown to expand upon exposure to 79.3% RH, as shown in Figures 9–11 and 13. However, this expansion was found to be quite sensitive to RH and, hence, the thickness of the adsorbed water layer on mica; the expansion was not significant at 71.2% and 100% RH (see Figure 14) or at 50–60% RH (Figure 6). Moreover, this conformational change of PMMA on mica is found to occur reversibly with a change of relative humidity between 79.3% and 100% RH.

Therefore, in this section we briefly discuss possible physical factors underlying these observations. An isolated PMMA chain is spread on water as a condensed monolayer in which parts of the chains take on loop-and-train configurations, as schematically shown in Figure 16a, where we also indicated the following interactions: (i) attractive interactions between the $-\text{COOCH}_3$ group and water, which tends to dissolve PMMA in water; (ii) repulsive interactions (hydrophobic interactions) between the backbone chain of PMMA and water, which tend to avoid dissolution of PMMA in water; and (iii) van der Waals attractive interactions between PMMA segments. From our observations, we expect that an isolated PMMA chain may form a condensed monolayer on water as a consequence of the force associated with force i being weaker than that associated with forces ii and iii.

Immediately after the transfer and deposition of PMMA onto mica in a very low relative humidity, the situation of the system is essentially identical to that shown in Figure 16a, except for the following two changes. One is a replacement of water by mica and the resulting changes in the interactions i

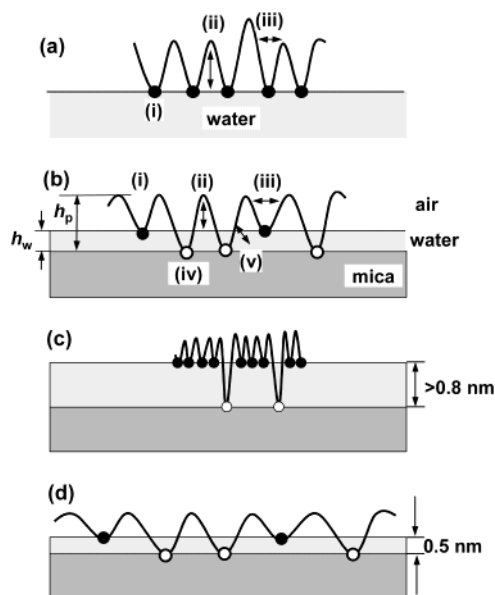


Figure 16. Schematic representation of PMMA block chains spread on water (a) and after transfer and deposit on mica with normal relative humidity of our laboratory (50–60% RH) with an adsorbed water layer of height h_w and PMMA monolayer of height h_p relative to the mica surface. The sketches in parts c and d are intended to show, respectively, the situations for 100% and 79.3% RH.

and ii. The other is the reduced mobility of PMMA chains on mica.

After exposing the system to relatively high humidity, the situation may be changed to one represented by Figure 16b. Some parts of the single chain will be floating on water, while others sections will be adhered to mica. The interactions i–iii in Figure 16b are identical to those in Figure 16a, while interactions iv and v are attractive between the $-\text{COOCH}_3$ group and mica, and repulsive (hydrophobic) between the PMMA backbone segments and water. The net attractive interactions between mica and PMMA may be determined by a balance of the attractions between mica and the $-\text{COOCH}_3$ group (iv), the attractions between PMMA segments (iii), and between water and the $-\text{COOCH}_3$ group (i) versus repulsions between water and the PMMA backbone (ii and v). This latter factor may depend on the height of the adsorbed water layer (h_w) and the PMMA layer (h_p) on mica. Increasing h_w causes increases

the repulsions ii and v, which results in reducing the net attractive interactions between mica and PMMA (iv) and enhancing mobility of PMMA chains on the mica surface, as well.

The large RH (e.g. 100% RH) with a large height h_w (>0.8 nm) may increase the repulsive interactions, which may then pull the chain out of the mica substrate surface onto the water surface in the form of a condensed monolayer, as schematically indicated in Figure 16c. This situation may be very similar to that of the isolated single PMMA chain on a water surface. However, decreasing RH (e.g. 79.3% RH) and hence decreasing h_w (≈ 0.5 nm) would decrease the repulsions (v) and increase adsorption of the $-\text{COOCH}_3$ groups onto mica. The increasing number of adsorbed sites of PMMA on mica, together with increased mobility of PMMA on mica driven by the weakened net attractive interactions between PMMA and mica mediated by the adsorbed water layer, may expand the PMMA chain conformation, as schematically shown in Figure 16d. However, at 71.2% RH (Figure 14a) or at 50–60% RH (RH of our laboratory) (Figures 5 and 6), the PMMA conformation on the water surface is expected to be kept unchanged on the mica surface, because h_w is small, and hence the attractions between PMMA and mica are strong and the mobility of PMMA is small.

4. Conclusion

We have developed a method to observe isolated single polymer chains on a two-dimensional surface by using AFM. The essential points for the success in the observation are as follows. The first is to use a block copolymer in order to

facilitate observation and identification of a single molecular chain; the PS monoblock particle isolated from others can be a target to find an isolated PMMA block chain emanating from the particle and to count the number of block copolymers on the mica surface. The second is to prepare the monolayer on a water surface from a very dilute solution of macromolecules and then transfer the monolayer onto a mica surface. The third is to expand the molecules deposited on mica under humid air. In this report, we used PS-*b*-PMMA as a model polymer to identify the single molecules. However, it is not necessary to use block copolymers; the technique should be applicable to a wide variety of polymers which are known to spread as monolayers on the water surface.^{22–25}

Acknowledgment. J.K. acknowledges Dr. Hiroshi Kiuchi, now retired from Toray Industries Inc., for giving him an opportunity to join the Hashimoto Polymer Phasing Project from Oct 1993 to Nov 1995. J.K. also sincerely appreciates Mr. Chiaki Tanaka, Toray Industries, Inc., for his support and encouragement throughout this work. We thank Mr. Yukihiro Nishikawa for technical assistance in a part of this work.

JA0290429

- (22) Gaines, G. L. *Insoluble Monolayers at Liquid–Gas Interfaces*; Interscience: New York, 1966.
- (23) Crisp, D. J. In *Surface Phenomena in Chemistry and Biology*; Danielli, Pankhurst, Riddiford, Eds.; Pergamon: London, 1958; pp 23–54.
- (24) Hironaka, S.; Koyama, M.; Ueno, M.; Meguro, K. *Hyoumen (Tokyo)* **1972**, *10*, 511–519; **1972**, *10*, 592–603; **1972**, *10*, 703–712; **1973**, *11*, 1–9.
- (25) Ulman, A. *An Introduction to Ultrathin Organic Films from Langmuir–Blodgett to Self-Assembly*; Academic Press: New York, 1991.